Magnetic circular x-ray dichroism of the 4d elements in disordered Co_xRh_{1-x} and Fe_xPd_{1-x} alloys

2001 J. Phys.: Condens. Matter 13 3895

(http://iopscience.iop.org/0953-8984/13/17/310)

INSTITUTE OF PHYSICS PUBLISHING JOURNAL OF PHYSICS: CONDENSED MATTER

J. Phys.: Condens. Matter **13** (2001) 3895–3906 www.iop.org/Journals/cm PII: S0953-8984(01)21487-8

Magnetic circular x-ray dichroism of the 4d elements in disordered Co_xRh_{1-x} and Fe_xPd_{1-x} alloys

S Ostanin[1], **V Popescu**[2] **and H Ebert**[2]

[1] Department of Physics and Astronomy, University of Glasgow, Glasgow G12 8QQ, UK
[2] Department Chemie/Physikalische Chemie,Universität München, Butenandtstrasse 5-13, D-81377 München, Germany

Received 29 January 2001, in final form 5 March 2001

Abstract

The magnetic properties of the disordered alloy systems face-centred-cubic (fcc) Co_xRh_{1-x} and fcc Fe_xPd_{1-x} have been investigated by means of the spin-polarized relativistic version of the Korringa–Kohn–Rostoker method of band-structure calculation on the basis of the coherent potential approximation alloy theory. In particular, the spin and spin–orbit-induced orbital magnetic moments have been calculated. In addition, the magnetic circular x-ray dichroism (MCXD) for the x-ray absorption coefficient has been determined. The relationship of the corresponding MCXD spectra and the magnetic moments of the absorber atom is discussed, with most emphasis put on the 4d element, whose magnetism is induced by the alloy partner.

1. Introduction

The magnetic circular x-ray dichroism (MCXD) in x-ray absorption—observed for the first time around a decade ago (Schütz *et al* 1987)—is now established as a tool for use in component-specific investigations of magnetic properties. At the beginning, measurements of this type were carried out in the hard-x-ray regime, e.g., at the K edge for the 3d elements (Schütz *et al* 1987, 1989a, Collins *et al* 1989) and at the $L_{2,3}$ edges for the 5d elements (Schütz *et al* 1989b). Later on, experiments in the technically more demanding soft-x-ray regime gave access to the $L_{2,3}$ edges of 3d elements and as a result it became possible to use MCXD to probe directly the 3d states which are the most important for transition metal magnetism (Chen *et al* 1990, van der Laan and Thole 1991).

For the 4d elements, MCXD experiments were first carried out at the $M_{2,3}$ edges (Harp *et al* 1994, 1995). These $M_{2,3}$ spectra are much less influenced by the core-hole lifetime broadening while obtaining the corresponding $L_{2,3}$ spectra is technically more demanding (Harp *et al* 1995). Nevertheless, such experiments are feasible now and accordingly there are quite a few experimental investigations on the MCXD of 4d elements to be found in the literature. Nearly all of this work has been devoted to two-component alloy (Harp *et al* 1994) or layered (Tomaz *et al* 1997, 1998) systems, aiming to investigate the 4d magnetism induced by the presence of a magnetic 3d element. This applies also to the investigations of Harp

0953-8984/01/173895+12$30.00

et al (1994, 1995) on the systems Fe_xRh_{1-x}, Co_xRh_{1-x} and Co_xRu_{1-x}. In particular, these authors investigated the question of whether the magnetic moments can be deduced from MCXD spectra on the basis of the so-called MCXD sum rules by carrying over the necessary information from related systems with known properties.

In the following, a corresponding theoretical study of the MCXD properties of the 4d elements in the alloy systems Co_xRh_{1-x} and Fe_xPd_{1-x} is presented.

The motivation of this work was twofold. On the one hand, the study of disordered alloys allows one to see the concentration as an independent parameter to be varied. Of course, MCXD is a perfect tool for monitoring the resulting induced magnetic moments of the 4d alloy partner. Furthermore, the theoretical study of completely disordered alloys supplies information on the effects of clustering on the onset of the ferromagnetism, which is an important issue in the case of Rh-rich Co_xRh_{1-x} alloys. On the other hand, the study of disordered alloys with fcc structure was extended by making calculations for tetragonally distorted and ordered compounds. This allowed us to investigate the influence of ordering and lattice distortion in some detail. In this way, it was possible to obtain information complementary to that from the previous work of Galanakis *et al* (2000), which was restricted to ordered and stoichiometric FePd compounds.

To get access to the spin–orbit-induced orbital magnetic moments and to properly account for all possible sources of the MCXD, all calculations to be presented were carried out in a fully relativistic way. Some computational details are summarized in the next section. Results for the magnetic moments and the MCXD spectra are presented in section 3. In discussing these data, the main emphasis will be put on the relation of the MCXD signal and the corresponding magnetic moments of the absorbing atom.

2. Computational details

As a first step of our investigations, the potentials for the various randomly disordered alloys were created self-consistently. This was done using the spin-polarized relativistic version of the Korringa–Kohn–Rostoker method of band-structure calculation in connection with the coherent potential approximation alloy theory (SPR-KKR–CPA) (Ebert *et al* 1992, Ebert 2000). The exchange and correlation were accounted for on the basis of the relativistic version of spin-density functional theory in its local approximation (LSDA) (MacDonald and Vosko 1979) using the parametrization of Vosko *et al* (1980). Using the plain LSDA to calculate spin–orbit-induced orbital moments (see below), it is often found that these are too small when compared to experiment. This deficiency of the LSDA may be removed by adding the orbital polarization (OP) correction, as has been suggested by Brooks (1985). For 4d transition metals, however, inclusion of the OP correction leads only to minor changes in the orbital moment. For this reason, no OP term has been added within the present calculations.

The spin and orbital magnetic moments to be presented below were obtained from the expressions (Ebert *et al* 1988)

$$\mu^{\alpha}_{\rm spin} = -\frac{\mu_{\rm B}}{\pi}\,{\rm Im\,Trace}\int^{E_{\rm F}} {\rm d}E \int {\rm d}^3r\ \beta\sigma_z G^{+}_{\alpha}(\vec{r},\vec{r},E) \tag{1}$$

$$\mu^{\alpha}_{\rm orb} = -\frac{\mu_{\rm B}}{\pi}\,{\rm Im\,Trace}\int^{E_{\rm F}} {\rm d}E \int {\rm d}^3r\ \beta l_z G^{+}_{\alpha}(\vec{r},\vec{r},E). \tag{2}$$

Here $G^{+}_{\alpha}(\vec{r},\vec{r},E)$ is the Green's function projected onto the alloy component α determined within the SPR-KKR–CPA formalism (Ebert 2000). All other quantities have their usual meaning; in particular, β is one of the standard Dirac matrices, σ_z is one of the 4×4 Pauli matrices and l_z is the z-component of the angular momentum operator (Rose 1961).

For the calculation of the corresponding x-ray absorption coefficients $\mu_\alpha^{\vec{q}\lambda}$ the expression

$$\mu_\alpha^{\vec{q}\lambda} \propto \sum_i \langle \phi_i | X_{\vec{q}\lambda}^\dagger | G^+ | X_{\vec{q}\lambda} | \phi_i \rangle \tag{3}$$

was used (Ebert 1996). Here i labels the various core states $|\phi_i\rangle$ involved and the Green's function $G_\alpha^+(\vec{r}, \vec{r}', E)$ projected onto the alloy component α represents the final states (Ebert 1996). Finally, the operator $X_{\vec{q}\lambda} = -e\vec{\alpha} \cdot \vec{A}_{\vec{q}\lambda}$, with $\vec{\alpha}$ the vector of the Dirac matrices, describes the interaction between the electronic current and the vector potential $\vec{A}_{\vec{q}\lambda}$ corresponding to radiation with polarization λ and wave vector $\vec{q}$.

For a direct comparison of the calculated absorption coefficient $\mu_\alpha^{\vec{q}\lambda}$ with experimental data, the corresponding theoretical spectra were broadened in the usual way. This means in particular that a Lorentzian broadening was applied to account for the finite lifetime of the core hole and excited electrons and a Gaussian broadening was used to represent the finite experimental resolution (Ebert 1996).

The outstanding feature of the absorption coefficients $\mu_\alpha^{\vec{q}\lambda}$ for circularly polarized radiation ($\lambda = +/-$ for left/right circular polarization) is that they enable one to deduce an estimate for the spin and orbital magnetic moments of the absorbing atom α from its dichroic spectrum $\Delta\mu_\alpha = \mu_\alpha^+ - \mu_\alpha^-$ defined as the difference of the absorption coefficients for left and right circularly polarized radiation. The corresponding analysis of the experimental spectroscopic data is based on the so-called MCXD sum rules (Wienke *et al* 1991, Thole *et al* 1992, Schütz *et al* 1993, Carra *et al* 1993). For an initial core state with p character, e.g., the $L_{2,3}$ edges, these are given by

$$\int (\Delta\mu_{L_3} - 2\,\Delta\mu_{L_2})\,\mathrm{d}E = \frac{N}{3N_h\mu_B}(\mu_{spin} + 7\mu_T) \tag{4}$$

$$\int (\Delta\mu_{L_3} + \Delta\mu_{L_2})\,\mathrm{d}E = \frac{N}{2N_h\mu_B}\mu_{orb}. \tag{5}$$

Here μ_T is the magnetic dipole moment, N is a normalization constant and N_h is the number of d holes. As discussed by many authors (for an overview see, for example, Ebert 1996) there are many problems connected with the application of the sum rules to experimental spectra—for example, fixing the energy range for integration or background subtraction, setting the number of holes N_h and the role of the term μ_T, to mention just the most serious ones. Nevertheless, they allow in general a rather reliable estimate for the spin and orbital moments of an absorbing atom to be obtained, that can be directly compared with theoretical results based on equations (1) and (2).

3. Results and discussion

3.1. The alloy system fcc Co_xRh_{1-x}

The low-temperature equilibrium structure of Co-rich disordered Co_xRh_{1-x} alloy is hcp while it is fcc on the Rh-rich side (Crangle and Parsons 1960). By rapidly cooling the high-temperature fcc phase it is however possible to obtain fcc samples also for the Co-rich side of the system. Accordingly, most experimental investigations on Co_xRh_{1-x} have been done on the (metastable) fcc phase. For the SPR-KKR–CPA calculations presented here, corresponding experimental data for the lattice parameters were used. The resulting spin and orbital magnetic moments are given in figure 1 in a component-resolved way. The calculated spin and orbital magnetic moments increase monotonically with decreasing Rh concentration with the Rh spin magnetic moment reaching a maximum of 0.5 μ_B for $x_{Rh} = 0.0$. As one notes, the system is theoretically found to be ferromagnetic throughout the whole concentration range. This is a

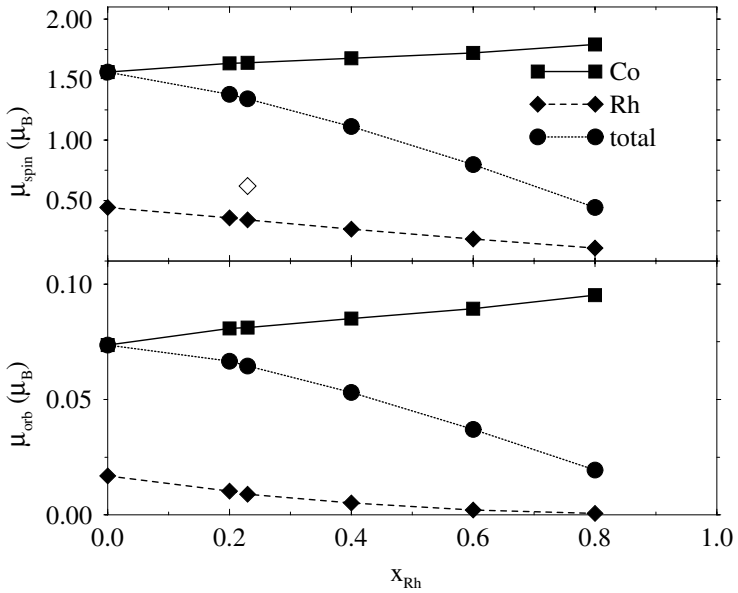

Figure 1. Spin (top) and orbital (bottom) magnetic moments of Co and Rh in disordered fcc Co_xRh_{1-x} alloys as calculated using the SPR-KKR–CPA method, using equations (1) and (2). The experimental value (open symbol) of Harp *et al* (1995) for the total magnetic moment $\mu_{Rh}^{tot} = \mu_{Rh}^{spin} + \mu_{Rh}^{orb}$ of Rh in $Co_{0.77}Rh_{0.23}$ has been added in the top panel.

direct consequence of the formation of a finite magnetic moment for Co atoms dissolved in Rh and the use of the CPA. Obviously, the CPA which is a so-called single-site mean-field theory is not able to account for the complex experimental situation on the Rh-rich side of the system. For $x_{Rh} > 0.8$, Co_xRh_{1-x} was found to be paramagnetic. In the region of $0.62 < x_{Rh} < 0.8$, the alloy system shows spin-glass behaviour and for higher Co concentrations it finally becomes ferromagnetic (Jamieson 1975).

As an application of the SPR-KKR–CPA formalism sketched above to the calculation of the MCXD, we show in figure 2 (top) the x-ray absorption spectra for the $M_{2,3}$ edges of Rh in $Co_{0.77}Rh_{0.23}$. These theoretical results are compared with corresponding experimental data recorded by Harp *et al* (1994, 1995). The spectra for unpolarized radiation can essentially be seen as a mapping of the 4d-like partial density of states of Rh. This means that the pronounced white line at the absorption edge is due to the unoccupied part of the broad 4d band complex of Rh. The broad shoulder at about 10 eV is a characteristic feature of XAS spectra of fcc metals (Ebert *et al* 1996), that primarily reflects the atomic coordination around the absorbing atom. As one can see in figure 2, all the above-mentioned features of the experimental spectrum are reproduced by the corresponding calculations. Furthermore, these give the spin–orbit splitting of the Rh 3p states as 24.843 eV, in excellent agreement with the experimental value, 24.8 eV (Fuggle and Inglesfield 1992).

The lower panel of figure 2 gives the circular dichroic spectrum $\Delta\mu_{M_{2,3}} = \mu^{+}_{M_{2,3}} - \mu^{-}_{M_{2,3}}$ of Rh in $Co_{0.77}Rh_{0.23}$. Obviously, there is a quite pronounced dichroic signal that is concentrated in the white-line region. This dichroic signal unambiguously proves the existence of a magnetic moment for the Rh atom that is induced by its ferromagnetic alloy partner.

Harp *et al* (1995) used their experimental MCXD spectra to deduce the total magnetic moment $\mu_{Rh}^{tot} = \mu_B(\langle\sigma_z\rangle + \langle l_z\rangle)$ making use of the integral form of the MCXD sum rules.

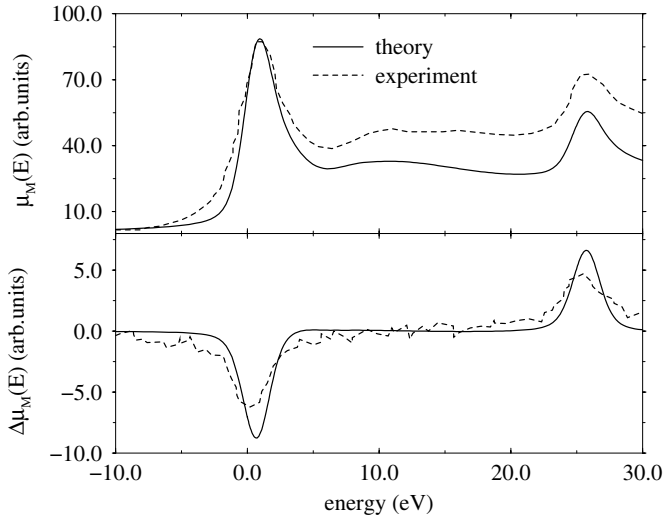

Figure 2. X-ray absorption spectra for the $M_{2,3}$ edges of Rh in $Co_{0.77}Rh_{0.23}$. Top: the absorption coefficient $\bar{\mu}_{M_{2,3}}$ for unpolarized radiation. Bottom: the difference of the absorption coefficients $\Delta\mu_{M_{2,3}} = \mu^{+}_{M_{2,3}} - \mu^{-}_{M_{2,3}}$ for left and right circularly polarized radiation. Theory: full lines; experiment: dashed lines (Harp *et al* 1994, 1995).

For $Co_{0.77}Rh_{0.23}$, Harp *et al* deduced for Rh a total magnetic moment of 0.62 μ_B. This is in reasonably good agreement with the calculated spin and orbital magnetic moments given in figure 1. Instead of exploiting the sum rules in full to investigate the spin and orbital moments separately (equations (4) and (5)), these authors considered the total moment. The reason for this is presumably the small signal-to-noise ratio of the experimental MCXD signal, which prevented them from giving reliable results for the expression $\Delta\mu_{M_3} - \Delta\mu_{M_2}$ entering equation (5). As for the work of Samant *et al* (1994), these authors assumed that the integral spectra can be normalized by a calibration factor taken from a system for which all relevant magnetic properties are known. This procedure in particular relies on the assumption that the variation of integral MCXD spectra is linearly dependent on the total magnetic moment. To test this property, the MCXD spectra of Rh in Co_xRh_{1-x} were calculated for several concentrations. Figure 3 gives these spectra normalized by the factor $\mu^{tot}_{Rh}(x_{Rh} = 0)/\mu^{tot}_{Rh}(x_{Rh})$. Obviously, the various curves coincide fairly well although the total magnetic moment μ^{tot}_{Rh} of Rh varies quite strongly with the concentration x_{Rh}. Nevertheless, one can see some deviations. First of all, one finds some differences in the line shape—in particular for the $x_{Rh} = 0$ spectrum. In addition, one notes that the minima of the various curves for $x_{Rh} \neq 0$ coincide quite well for the M_3 edge while there is a rather appreciable spread for the maxima at the M_2 edge. Results similar to those shown in figure 3 have been obtained recently by Alouani *et al* (1998) for the $L_{2,3}$-edge spectra of Fe in several Fe nitride compounds. One can therefore say that the assumption of a proportionality between the integral MCXD spectra and the total magnetic moment of the absorbing atom is reasonably well justified and allows a rather reliable estimation of the magnetic moment on the basis of the MCXD sum rules.

An investigation on the MCXD at the $L_{2,3}$ edges of Rh in Co_xRh_{1-x} alloys has been performed recently by Grange and co-workers (Grange 1999). The spectra recorded by these authors are shown in figure 4. As could be expected from a previous theoretical study (Ebert 1997), apart from the different spin–orbit splitting of the p-like core states, the $L_{2,3}$-edge spectra do not noticeably differ from those for the $M_{2,3}$ edges. One notes that the theoretical

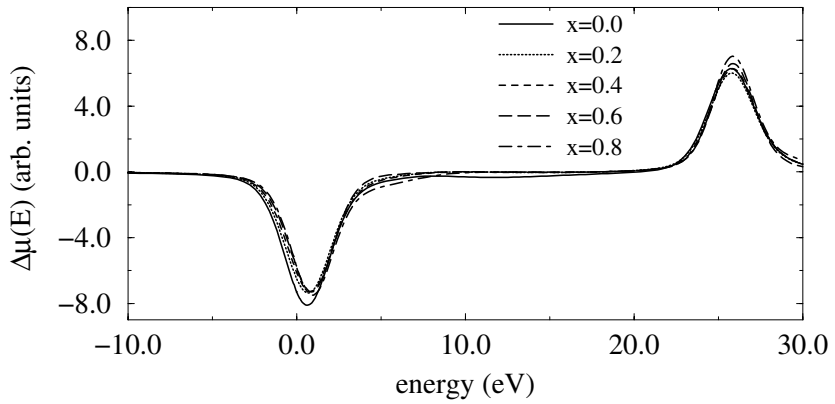

Figure 3. Theoretical MCXD spectra for the $M_{2,3}$ edges of Rh in $Co_{1-x}Rh_x$. The spectra have been normalized by a factor of $\mu^{tot}_{Rh}(x_{Rh} = 0)/\mu^{tot}_{Rh}(x_{Rh})$ with μ^{tot}_{Rh} the total magnetic moment of Rh.

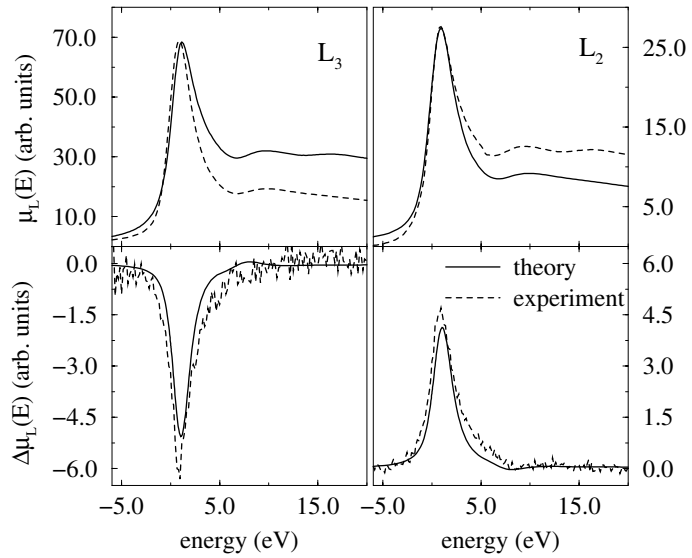

Figure 4. X-ray absorption spectra for the L_2 edge (right) and the L_3 edge (left) of Rh in $Co_{0.77}Rh_{0.23}$. Top: the absorption coefficient $\bar{\mu}_{L_{2,3}}$ for unpolarized radiation. Bottom: the difference of the absorption coefficients $\Delta\mu_{L_{2,3}} = \mu^{+}_{L_{2,3}} - \mu^{-}_{L_{2,3}}$ for left and right circularly polarized radiation. Theory: full lines; experiment: dashed lines (Grange 1999).

$L_{2,3}$ spectra included in figure 4 show a very satisfactory agreement with the experimental ones. In particular, the MCXD spectra are properly reproduced by the calculations.

The pronounced spin polarization of the 4d component by its 3d alloy partner is a common feature of many other 3d–4d transition metal systems, and can be attributed to the 3d–4d hybridization and exchange interactions (Vogel *et al* 1997). These also have important consequences for many other magnetic properties—for example, the magnetocrystalline anisotropy energy (Solovyev *et al* 1995) which is often found to be enhanced compared to that of the pure 3d transition metal. A prominent example showing this is the alloy system Fe_xPd_{1-x}.

3.2. The alloy system fcc Fe_xPd_{1-x}

During recent years intensive experimental as well as theoretical studies were devoted to the alloy system fcc Fe_xPd_{1-x}; these were primarily motivated by the increasing range of its technological applications, which mainly arose because of the giant magnetic anisotropy that occurs in Fe_xPd_{1-x} alloys and multilayers. Indeed, the SPR-KKR–CPA calculations gave for the binary alloy Fe_xPd_{1-x} a strong spin polarization induced on the Pd atom and an enhancement of the Fe magnetic moments compared to those in pure Fe or Fe 3d alloys. Because of the common lattice structure, one might expect the Fe_xPd_{1-x} system to exhibit magnetic characteristics similar to those of Co_xRh_{1-x}. However, if one looks at the concentration dependence of the magnetic moments of Fe and Pd shown in figure 5, several differences can be clearly seen when comparing with the corresponding curves for Co_xRh_{1-x} (see figure 1). In contrast to the case for Rh in Co_xRh_{1-x}, the induced spin and orbital moments of Pd rapidly increase when Fe is added to Pd and have already reached their maximum values at around $x_{Pd} = 0.8$. For lower Pd concentrations the spin as well as the orbital moments are almost concentration independent. This behaviour is fully in line with results of neutron diffraction experiments on Fe_xPd_{1-x} (Cable *et al* 1965). These gave a Pd magnetic moment that is nearly constant ($\mu_{spin} = 0.35\ \mu_B$) over a wide range of concentrations, i.e., it has the same behaviour as that found by the present SPR-KKR–CPA calculations. One should also mention here that our results for the disordered alloy $Fe_{0.5}Pd_{0.5}$ are rather close to those calculated by Solovyev *et al* (1995) for the ordered compound FePd. On the other hand, while the orbital moments of Pd are about double those of Rh in Co_xRh_{1-x}, the spin moments are half the size. At first sight this might seem surprising, since the alloy partner of Pd has a larger spin moment than that of Rh in Co_xRh_{1-x} alloys.

The first investigations on the MCXD for the $L_{2,3}$ edges of Pd in disordered Fe_xPd_{1-x} alloys were carried out by Kobayashi *et al* (1996). Recently, measurements of the MCXD at

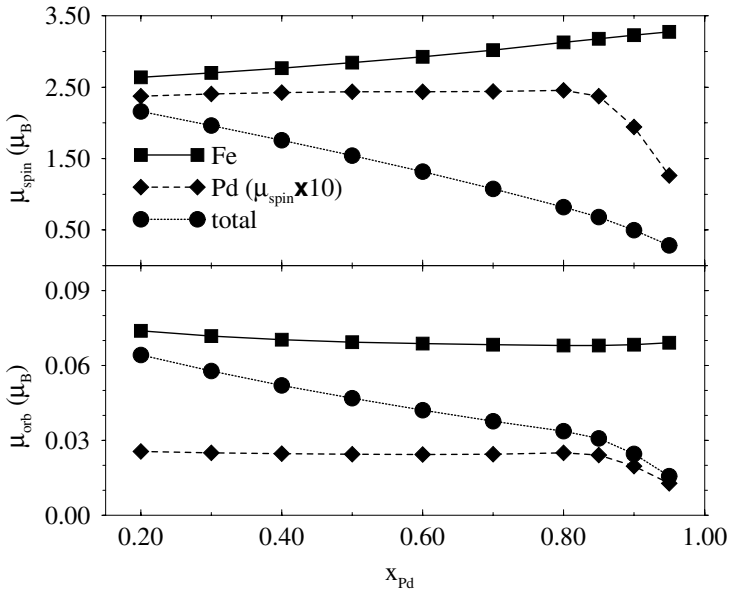

Figure 5. Spin (μ_{spin}) and orbital (μ_{orb}) magnetic moments (in Bohr magnetons μ_B) of Fe and Pd in Fe_xPd_{1-x} alloys calculated using the SPR-KKR–CPA method, using equations (1) and (2). The corresponding values per formula unit were added.

the $L_{2,3}$ edges of Pd in Pd/Fe multilayers (Vogel *et al* 1997) and in $Fe_{0.5}Pd_{0.5}$ alloy films (Kamp *et al* 1999) were also reported. Figure 6 shows the results of Kobayashi *et al* for $x_{Pd} = 0.403$ and $x_{Pd} = 0.671$ compared with theoretical spectra obtained using the approach sketched above. The corresponding calculations were performed for $x_{Pd} = 0.40$ and $x_{Pd} = 0.70$, values that are close enough to allow a direct comparison. An overall reasonable agreement between the theoretical and experimental spectra can be noticed for these systems, showing the expected similarities in electronic structure with the Co_xRh_{1-x} alloys. The more pronounced difference in amplitude of the dichroic signal for the L_2 and L_3 edges predicted by our calculations compared with the results for Rh in Co_xRh_{1-x} (see figures 2–4) is a direct consequence of the larger orbital moment on the Pd site (see figures 1 and 5). Applying the sum rule in equation (5), Kobayashi *et al* (1996) found a nearly vanishing orbital moment for Pd and concluded that this seems to be quenched. However, recently Vogel *et al* (1997) and Kamp *et al* (1999) deduced from their MCXD investigations on Fe_xPd_{1-x} an orbital moment for Pd of the same magnitude as the SPR-KKR–CPA calculation results. The discrepancy with the results of Kobayashi *et al* can be explained by recalling that this system shows a pronounced perpendicular magnetic anisotropy. The experimental spectra presented in figure 6, on the other hand, were recorded with a magnetic field applied in the plane (Kobayashi *et al* 1996). Moreover, theoretical investigations similar to those whose results are shown in figure 3 were performed also for the $L_{2,3}$ edges of Pd in Fe_xPd_{1-x} and an identical behaviour (hence, not reproduced here) was obtained. As a consequence one may again conclude that reliable estimates for the magnetic moments can be obtained on the basis of the MCXD sum rules.

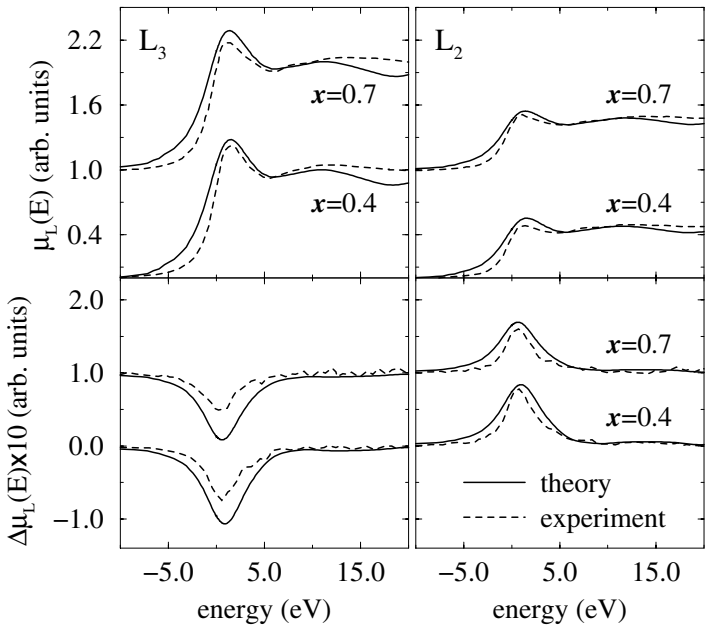

Figure 6. X-ray absorption spectra for the L_2 edge (right) and L_3 edge (left) of Pd in Fe_xPd_{1-x} for $x_{Pd} = 0.40$ and $x_{Pd} = 0.70$. Top: the absorption coefficient $\bar{\mu}_{L_{2,3}}$ for unpolarized radiation. Bottom: the difference of the absorption coefficients $\Delta\mu_{L_{2,3}} = \mu^{+}_{L_{2,3}} - \mu^{-}_{L_{2,3}}$ for left and right circularly polarized radiation. Theory: full lines; experiment: dashed lines (Kobayashi *et al* 1996). All the spectra related to $x_{Pd} = 0.70$ are shifted vertically. The experimental concentrations slightly deviate from those used in the calculations, i.e., they correspond to $x_{Pd} = 0.403$ and $x_{Pd} = 0.671$.

3.3. The bulk $Fe_{0.5}Pd_{0.5}$ alloy

The bulk $Fe_{0.5}Pd_{0.5}$ alloy exhibits at 920 K a phase transition from the low-temperature disordered γ-phase having a fcc structure to an ordered $L1_0$ tetragonal structure characterized by a strong perpendicular magnetic anisotropy (Gehanno *et al* 1997). Thin films of $Fe_{0.5}Pd_{0.5}$ alloys deposited by molecular beam epitaxy on the different substrates can adopt the $L1_0$ tetragonal phase with lattice parameters depending on the preparation conditions and the growth temperature (Kamp *et al* 1999, Boeglin *et al* 1999).

Kamp and co-workers (Kamp *et al* 1999) have investigated the influence of chemical ordering on the MCXD for the $L_{2,3}$ edges of Pd and Fe in $Fe_{0.5}Pd_{0.5}$ alloy films. The MCXD in this alloy system was found to be rather sensitive to the changes in the chemical order (Kamp *et al* 1999) as seen from variations in the spin and orbital magnetic moments extracted from the experimental spectra via the MCXD sum rules. The Fe spin moment obtained within these investigations decreases with chemical ordering from 2.13 μ_B to 2.04 μ_B, while the orbital Fe magnetic moment increases from 0.22 μ_B to 0.42 μ_B with increasing degree of order in $Fe_{0.5}Pd_{0.5}$ (Kamp *et al* 1999). Hence, as the MCXD sum rules indicate, the Fe spin magnetic moments are smaller than those for pure Fe, whereas the orbital magnetic moments on the Fe site are strongly enhanced compared to the experimental value for pure Fe ($0.19\mu_B$). Kamp *et al* (1999) reported quite large induced moments for Pd: 0.58 ± 0.03 μ_B and 0.038 ± 0.005 μ_B for the spin and orbital magnetic moments, respectively. Macroscopic SQUID measurements on $Fe_{0.5}Pd_{0.5}$ give an average magnetic moment/atom of 1.46 ± 0.15 μ_B (Kamp *et al* 1999).

Using the full-potential linear muffin-tin orbital method, Galanakis *et al* (2000) calculated the structural and magnetic properties of the ordered FePd compound having a tetragonally distorted CuAu structure. These authors reported that the Fe spin magnetic moment increases slightly from 2.92 μ_B to 2.96 μ_B if c/a is varied from 1 to 0.938. The latter value corresponds to the sample of Kamp *et al* that showed the highest degree of order, with about 95% of the atoms sitting on their proper lattice sites (Kamp *et al* 1999). The Pd spin magnetic moment of 0.34 μ_B obtained for $c/a = 1$ increases slightly by 0.01 μ_B due to the lattice distortion. This theoretical result is in good agreement with previous calculations for ordered FePd by other authors (Solovyev *et al* 1995, Moruzzi and Marcus 1993). The calculations of Galanakis and co-workers (Galanakis *et al* 2000) were done using plain LSDA as well as including an additional OP correction as suggested by Brooks (1985). Including the OP term, the values 0.073 μ_B and 0.026 μ_B were obtained for the orbital magnetic moments of Fe and Pd, respectively, in ordered FePd for $c/a = 0.938$. These theoretical orbital magnetic moments are only slightly higher than for undistorted ordered FePd with $c/a = 1$ and seem to be too small when compared with the results of Kamp *et al* (1999). This is also reflected by the deviation of the MCXD spectra calculated by Galanakis *et al* (2000) from their experimental counterparts.

To investigate the influence of ordering and lattice distortions on the magnetic properties of the system Fe–Pd in more detail, the SPR-KKR technique was applied to ordered FePd for $c/a = 1$ and 0.938, as was also done by Galanakis *et al* (2000). In addition, calculations were made for disordered $Fe_{0.5}Pd_{0.5}$ having fcc and fct ($c/a = 0.938$) structure, making use of the CPA. The resulting spin and orbital magnetic moments are collected in table 1. As one can see, our results for ordered FePd are in good agreement with those of Galanakis *et al* (2000). The Fe and Pd spin magnetic moments increase under uniaxial stress compared with those for $c/a = 1$, reaching the values of 2.77 μ_B and 0.33 μ_B, respectively. As one might expect, disorder has an opposite effect. While the Fe spin moment decreases slightly, the induced Pd spin moment goes down to 0.25 μ_B. This value is very close to that for Pd in ordered undistorted FePd with $c/a = 1$. The Fe and Pd orbital magnetic moments in the

Table 1. Spin, orbital and total magnetic moments (in Bohr magnetons, μ_B) for the ordered FePd and disordered $Fe_{0.5}Pd_{0.5}$ calculated within the SPR-KKR–CPA scheme, using equations (1) and (2).

	FePd	$Fe_{0.5}Pd_{0.5}$	FePd	$Fe_{0.5}Pd_{0.5}$
c/a	1.000	1.000	0.938	0.938
Fe μ_{spin}	2.68	2.84	2.77	2.74
Pd μ_{spin}	0.27	0.24	0.33	0.25
Fe μ_{orb}	0.08	0.069	0.074	0.06
Pd μ_{orb}	0.024	0.024	0.024	0.022
μ_{tot}/atom	1.470	1.544	1.558	1.497

ordered FePd alloys show only minor changes due to strain while the disorder effect in the fct Fe_xPd_{1-x} system gives rise to a small decrease. This is in qualitative agreement with the experimental data for the orbital magnetic moments μ_{orb} extracted from the MCXD spectra via the sum rules (Kamp *et al* 1999). The discrepancy concerning the effect of ordering between our calculated spin magnetic moments in $Fe_{0.5}Pd_{0.5}$ and the experimental MCXD results of Kamp *et al* (1999) might be caused by problems due to the complex film specimen used in the experiment. The total magnetic moment of 1.47 μ_B/atom, calculated for ordered and undistorted FePd, increases firstly up to $\sim$1.56 μ_B/atom under distortion and then, when the CPA is applied to the disordered fct Fe_xPd_{1-x} system, decreases to the value $\sim$1.5 μ_B/atom, which is close to the result of SQUID measurements.

The calculated $L_{2,3}$ MCXD spectra for the Fe site in the ordered FePd and disordered fct $Fe_{0.5}Pd_{0.5}$ are shown in figure 7 along with the measured MCXD spectrum of the ordered sample of Kamp *et al* (1999). The calculations were done for the lattice parameters corresponding to the experimental samples. The experimental and calculated MCXD spectra in figure 7 have been aligned with respect to the energy axis by bringing the L_3 peak to coincidence. There is excellent agreement concerning the peak positions and the relative intensities between experiment and our theoretical result for the ordered distorted compound. The predicted L_2 MCXD intensity obtained for the disordered alloy is higher than that observed in experiment. These findings are not surprising, because the Fe orbital magnetic moment increases with chemical ordering. Finally, the small deviations of the calculated MCXD spectrum for ordered FePd from its experimental counterpart can be attributed to shortcomings of our bulk model as regards describing the more complicated experimental situation for the thick-film geometry.

4. Summary

The magnetic properties of the disordered alloy systems fcc Co_xRh_{1-x} and fcc Fe_xPd_{1-x} have been investigated by means of the fully relativistic SPR-KKR–CPA band-structure scheme. This approach allowed us in particular to obtain the spin–orbit-induced orbital magnetic moments. In addition, the x-ray absorption spectra for these disordered alloys were calculated. The fully relativistic scheme applied led to a proper description of the spin–orbit-induced MCXD for the various 3d and 4d transition metals involved. In particular, these calculations were able to confirm the magnetization induced in the 4d transition metals by their alloy partners. Comparison with experimental data led to a rather satisfactory agreement in all cases. From this one may conclude that the MCXD sum rules supply reliable estimates for the component-resolved spin and orbital moments.

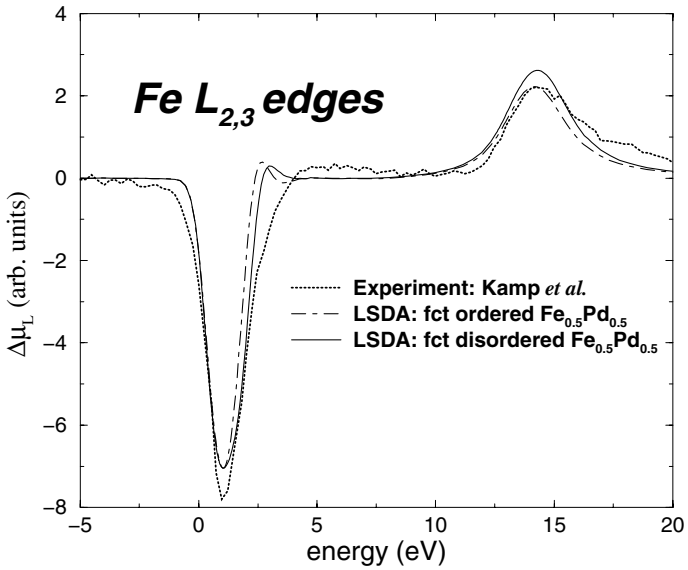

Figure 7. Theoretical MCXD spectra for the Fe $L_{2,3}$ edges in the chemical ordered and disordered fct $Fe_{0.5}Pd_{0.5}$ alloys compared with the experimental result of Kamp *et al* (1999). The theoretical MCXD spectra have been normalized to the L_3 absorption peak.

We have also shown that the same theoretical approach can be successfully applied to the MCXD findings for the distorted 3d–4d binary alloys. For instance, the MCXD spectra calculated for tetragonal $Fe_{0.5}Pd_{0.5}$ show good agreement with the observed ones. While the XAS excitation probes the $L_{2,3}$ edges at the 3d site, which show a rather strong MCXD signal compared to the 4d partner in these alloys, the corresponding MCXD shape changes its form and the L_2:L_3 ratio with chemical ordering. Combining the theoretical technique proposed here with the experiments exploring the MCXD, one could find a new characterization probe for chemical ordering in film specimens—prepared, e.g., by molecular beam epitaxy—that might be disordered and stressed tetragonally. It would also give a very promising tool for studying the film binary systems with perpendicular magnetic anisotropy.

Acknowledgments

This work was supported by the German ministry for education and research (BMBF) under the contract 05 621WMA 9 within the programme *Zirkular polarisierte Synchrotronstrahlung: Dichroismus, Magnetismus und Spinorientierung* and the European TMR Network on *Ab Initio Calculations of Magnetic Properties of Surfaces, Interfaces and Multilayers*.

References

Alouani M, Wills J M and Wilkins J W 1998 *Phys. Rev.* B **57** 9502
Boeglin C, Bulou H, Hommet J, Cann X L, Magnan H, Fevre P L and Chandesris D 1999 *Phys. Rev.* B **60** 4220
Brooks M S S 1985 *Physica* B **130** 6
Cable J W, Wollan E O and Koehler W C 1965 *Phys. Rev.* **138** A755
Carra P, Thole B T, Altarelli M and Wang X 1993 *Phys. Rev. Lett.* **70** 694
Chen C T, Sette F, Ma Y and Modesti S 1990 *Phys. Rev.* B **42** 7262
Collins S P, Cooper M J, Brahmia A, Laundy D and Pitkanen T 1989 *J. Phys.: Condens. Matter* **1** 323

Crangle J and Parsons D 1960 *Proc. R. Soc.* A **255** 509
Ebert H 1996 *Rep. Prog. Phys.* **59** 1665
Ebert H 1997 *J. Physique Coll.* **7** C2 161
Ebert H 2000 *Electronic Structure and Physical Properties of Solids (Springer Lecture Notes in Physics vol 535)* ed H Dreyssé (Berlin: Springer) p 191
Ebert H, Drittler B and Akai H 1992 *J. Magn. Magn. Mater.* **104–107** 733
Ebert H, Stöhr J, Parkin S S P, Samant M and Nilsson A 1996 *Phys. Rev.* B **53** 16 067
Ebert H, Strange P and Gyorffy B L 1988 *J. Phys. F: Met. Phys.* **18** L135
Fuggle J C and Inglesfield J E (ed) 1992 *Unoccupied Electronic States (Springer Topics in Applied Physics vol 69)* (New York: Springer)
Galanakis I, Ostanin S, Alouani M, Dreysse H and Wills J 2000 *Phys. Rev.* B **61** 599
Gehanno V, Marty A, Gilles B and Samson Y 1997 *Phys. Rev.* B **55** 12 552
Grange W 1999 *PhD Thesis* University of Strasbourg
Harp G R, Parkin S S P, O'Brien W L and Tonner B P 1994 *J. Appl. Phys.* **76** 6471
Harp G R, Parkin S S P, O'Brien W L and Tonner B P 1995 *Phys. Rev.* B **51** 12 037
Jamieson H C 1975 *J. Phys. F: Met. Phys.* **5** 1021
Kamp P, Marty A, Gilles B, Hoffmann R, Belakhovsky M, Boeglin C, Dürr H A, Dhesi S S, van der Laan G and Rogalev A 1999 *Phys. Rev.* B **59** 1105
Kobayashi K, Maruyama H, Iwazumi T, Kawamura N and Yamazaki H 1996 *Solid State Commun.* **97** 491
MacDonald A H and Vosko S H 1979 *J. Phys. C: Solid State Phys.* **12** 2977
Moruzzi V L and Marcus P M 1993 *Phys. Rev.* B **48** 16 106
Rose M E 1961 *Relativistic Electron Theory* (New York: Wiley)
Samant M G, Stöhr J, Parkin S S P, Held G A, Hermsmeier B D, Herman F, van Schilfgaarde M, Duda L C, Mancini D C, Waasdahl N and Nakajima R 1994 *Phys. Rev. Lett.* **72** 1112
Schütz G, Frahm R, Wienke R, Wilhelm W, Wagner W and Kienle P 1989a *Rev. Sci. Instrum.* **60** 1661
Schütz G, Knülle M and Ebert H 1993 *Phys. Scr.* T **49** 302
Schütz G, Wagner W, Wilhelm W, Kienle P, Zeller R, Frahm R and Materlik C 1987 *Phys. Rev. Lett.* **58** 737
Schütz G, Wienke R, Wilhelm W, Wagner W, Kienle P, Zeller R and Frahm R 1989b *Z. Phys.* B **75** 495
Solovyev I V, Dederichs P H and Mertig I 1995 *Phys. Rev.* B **5** 13 419
Thole B T, Carra P, Sette F and van der Laan G 1992 *Phys. Rev. Lett.* **68** 1943
Tomaz M A, Ingram D C, Harp G R, Lederman D, Mayo E and O'Brien E L 1997 *Phys. Rev.* B **56** 5474
Tomaz M A, Mayo E, Lederman D, Hallin E, Sham T K, O'Brien W L and Harp G R 1998 *Phys. Rev.* B **58** 11 493
van der Laan G and Thole B T 1991 *Phys. Rev.* B **43** 13 401
Vogel J, Fontaine A, Cros V, Petroff F, Kappler J P, Krill G, Rogalev A and Goulon J 1997 *J. Magn. Magn. Mater.* **165** 96
Vosko S H, Wilk L and Nusair M 1980 *Can. J. Phys.* **58** 1200
Wienke R, Schütz G and Ebert H 1991 *J. Appl. Phys.* **69** 6147